Seismic assessment of unreinforced masonry structures: a coupled mesoscale-DMEM approach

Vadalà Federica* - Department of Civil Engineering, University of Minho, ISISE, Guimarães, Portugal, e-mail: federicavadala03@gmail.com

Cusmano Valeria - Department of Civil Engineering and Architecture (DICAR) University of Catania, Catania, Italy, e-mail: valeria.cusmano@phd.unict.it

Szabó Simon - Department of Civil Engineering, University of Minho, ISISE, Guimarães, Portugal, e-mail: simon.szabo117@gmail.com

Funari Marco Francesco - Department of Civil Engineering, University of Minho, ISISE, Guimarães, Portugal, e-mail: marcofrancesco.funari@civil.uminho.pt

da Silva Luis C.M. - Department A.B.C., Politecnico di Milano, Piazza Leonardo da Vinci 32, 20133 Milan, Italy, e-mail: Luiscarlos.martinsdasilva@polimi.it

Caliò Ivo – Department of Civil Engineering and Architecture (DICAR) University of Catania, Catania, Italy, e-mail: ivo.calio@unict.it

Lourenço Paulo B.- Department of Civil Engineering, University of Minho, ISISE, Guimarães, Portugal, e-mail: pbl@civil.uminho.pt

Abstract: A numerical investigation is performed to investigate the potential of a discrete macro-element coupled with a mesoscale approach for the seismic assessment of unreinforced masonry structures. At first, parametric analyses are performed on a U-shape stone masonry prototype. Nonlinear static analyses are performed to investigate parameters that affect the results when a mesoscale masonry pattern representation is adopted. Results prove the suitability of a mesoscale representation of unreinforced masonry structures through a discrete macro-element approach. Furhthermore, it is demonstrated that an irregular placement of masonry units' have a significant role in the structural response, either from a strength and ductility standpoints, when compared to a regular and periodic distribution of units.

Keywords: Unreinforced masonry structures; Mesoscale representation; Irregular masonry pattern, Discrete Macro-Element Method (DMEM)

1. Introduction

Several advanced analysis methods for the seismic assessment of unreinforced masonry (URM) structures were developed in the last decades (de Felice et al., 2010; Fortunato et al., 2017; P B Lourenço et al., 2022; Malena et al., 2019; Sharma et al., 2021). These are generally classified as numerical or analytical approaches (D'Altri et al., 2020; Karimzadeh et al., 2020). Analytical approaches can be based on limit analysis theorems, which have the great advantage of being simple to use and independent of most material properties, but assume simplified constitutive relathionships (Cascini et al., 2020; De Felice & Giannini, 2001; Funari et al., 2021). More sophisticated numerical approaches are typically implemented in the Finite Element Method (FEM) (Funari et al., 2021; Silva et al., 2018; Szabó et al., 2021) or Discrete Element Method (DEM) (Bui et al., 2017; Lemos, 2019) frameworks. FEM allows a more versatile application as masonry can be represented either through a homogeneous equivalent media (macro-modelling) or by a discrete representation of units and joints (micro-modelling). DEM is well suited for masonries with both dry- and mortared joints but still requires a full representation of the arrangement of the blocks

(Sarhosis et al., 2019; Savalle et al., 2020, 2022). Despite their reliability, the computational efficiency of the available numerical methods is rarely compatible with the need to have a rigorous real-time post-earthquake assessment (Funari et al., 2020; Funari et al., 2020; Lourenço & Silva, 2020). Therefore, several authors proposed alternative approaches to satisfy the need to have reliable results in relatively short computational times. Because of their simplicity and efficiency, these approaches are widely used also in engineering practice (L. C. M. da Silva & Milani, 2022; Marco F. Funari et al., 2022; Malomo & DeJong, 2021; Maria D'Altri et al., 2021; L. C. Silva et al., 2020)

In this framework, macro-element approaches were proposed in which structures are described as an assemblage of macroscopic structural elements. The Equivalent Frame Model (EFM) belongs to macro-model based strategies, and national and international standards are adopting it in combination with nonlinear static analysis (Quagliarini et al., 2017). Because of its simplicity and low computational cost, it is one of the most widely adopted analysis methods in engineering practice (Siano et al., 2018). Nevertheless, it presents some limitations, such as the difficulty of discretising structures with an irregular position of openings.

In order to cover such limitations and keep the computational efficiency, a discrete macro-element method designated as DMEM was proposed by (Caliò et al., 2012). DMEM allows the simulation of both the in-plane (IP) and out-of-plane (OOP) response of masonry walls. Such an approach has been proposed and validated in the nonlinear static field (Caliò et al., 2012) and extended to dynamics (Chácara et al., 2017). Nevertheless, further investigation on the influence of the macro-elements discretisation are required. Under this scope, the novelty of the study includes the application of a mesoscale masonry irregular pattern representation through DMEM. These allowed to the paper to: i) apply the DMEM approach by adopting a mesh representation consistent with real masonry patterns, and ii) evaluate how certain geometrical features of the masory arrangement affect the structural response.

2. The Discrete Macro-Element Method

DMEM approach was first developed by Caliò et al. (2012), and it was based on a basic plane element whose kinematics is dependent on four Lagrangian parameters only (three degrees of freedom associated to the in-plane rigid-body motion and an additional degree of freedom related to shear deformability in its own plane). This simple plane element Fig. 1a can be represented with a simple mechanical scheme constituted by an articulated quadrilateral with rigid edges connected at the vertices by four hinges and with two diagonal springs connected to the corners to simulate the shear behaviour. Each element interacts with the adjacent ones by means of a discrete distribution of a set of transversal nonlinear springs and a single sliding nonlinear spring, denoted as interfaces, which governs the flexural and sliding behaviour. However, this simple element can only simulate the nonlinear behaviour of masonry panels in their own plane, not considering the out-of-plane response. To overcome this limitation, two subsequent upgrades were performed to improve the potential of the approach. First, the OOP behaviour was considered by introducing additional rows of transversal nonlinear links and two additional OOP sliding links (able to govern the OOP shear sliding behaviour and the torsion), thus enabling the needed OOP degrees of freedoms (Fig. 1b). The number of orthogonal links is selected in accordance with the desired level of accuracy of the linear and nonlinear response. The shear deformability is still governed by a diagonal nonlinear link that connects two opposite corners of the articulated quadrilateral. A further upgrade was introduced considering a shell macro-element (Fig. 1c) characterised by an irregular geometry, variable thickness, and the element and skew interface to model complex curved geometry such as arches, vaults, and domes (Cannizzaro et al., 2018).

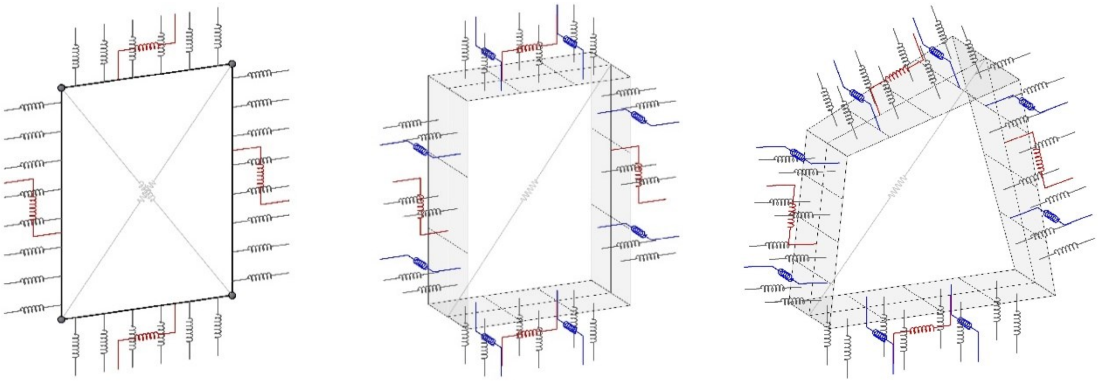

(a) (b) (c)

Fig. 1: DMEM evolution (a) Plane Element; (b) Regular Spatial Element; and (c) Irregular Spatial Element.

Details on the calibration procedures can be found in Pantò et al. (2017).
The reduced number of DOFs associated with each macro-element makes this approach computationally inexpensive if compared with the classical finite element formulations. DMEM approach classical interpretation implies that each macro-element must be representative of the corresponding finite portion of masonry walls, according to the macro-modelling approach. Even though DMEM is conceived as a macro-modelling strategy, there is the possibility to extend the discretisation at mesoscale representation. Nevertheless, depending on whether a macro- or mesoscale approach is adopted, it is necessary to appropriately calibrate the main mechanical parameters that influence the response as with mesoscale strategies, some physical phenomena can be described in more detail, i.e. interlocking effect between the blocks or the presence of well-defined and realistic fracture surfaces at the interface.

3. Numerical Investigation: U-shape stone

In this section, the effect of the mesh discretisation on the numerical simulations performed with the DMEM approach is assessed by means of parametric studies. The numerical investigation has been carried out on a simple structure of three walls forming a U-plan made of stone masonry, which idealises the experimental tests performed at the LNEC shaking table (Candeias et al., 2017). Fig. 2 reports the geometrical features of the masonry prototype.

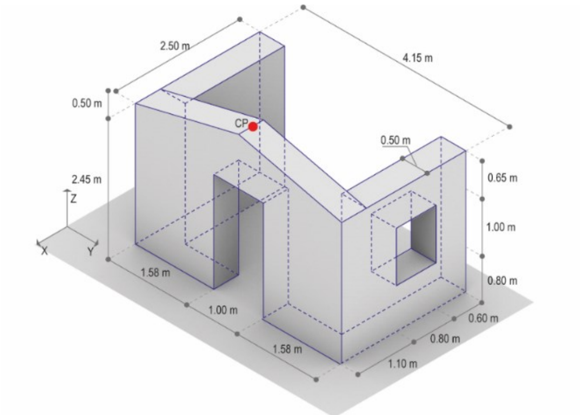

Fig. 2: Geometrical characteristics of the U-Shape stone prototype.

Four discretisations were adopted for the prototype geometry and are given in Fig. 3. In particular, M1, M2, and M3 are macroscale discretisations where the characteristic dimension of the elements is gradually decreased to reach three different levels of refinement. Regarding M4, a mesoscale discretisation was adopted in agreement with the one of Cannizzaro & Lourenço (2016).

Macroscale-: M1 **Macroscale: M2** **Macroscale: M3** **Mesoscale: M4**

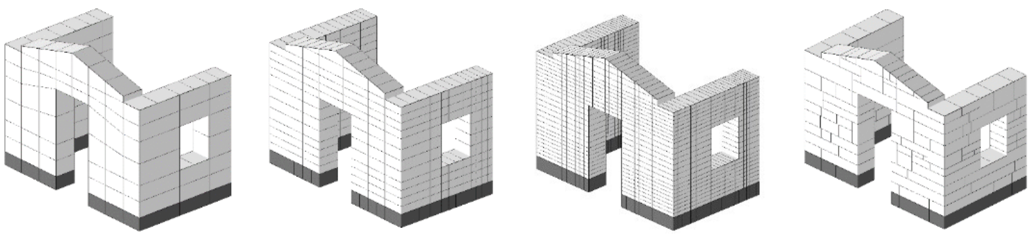

Fig. 3: Mesh discretisations adopted for the numerical investigations.

The definition of the mechanical properties has been initially conducted by assuming the same parameters adopted in Cannizzaro & Lourenço (2016) for all mesh discretisations (Table 1 and Table 2). It is worth underlining that when a mesoscale representation is adopted (M4), a linear-elastic constitutive law has been selected for the diagonal shear behaviour to avoid that diagonal cracking involves the single macro element. This assumption ensures that the shear failure does not occur when macro-element represents a single masonry unit (Vadalà et al., 2022).

Table 1: Mechanical properties adopted for the U-shape prototype: flexural behaviour (Cannizzaro & Lourenço, 2016).

	Flexural behaviour					
	Density	**Young's modulus**	**Compressive strength**	**Compressive fracture energy**	**Tensile strength**	**Tensile fracture energy**
Model	**[kg/m^3]**	**[MPa]**	**[MPa]**	**[N/mm]**	**[MPa]**	**[N/mm]**
M1,M2,M3	2360	2077	5.44	∞	0.224	0.048
M4	2360	2077	5.44	∞	0.224	0.048

Table 2: Mechanical properties adopted for the U-shape prototype: shear behaviour (Cannizzaro & Lourenço, 2016).

	Diagonal cracking behaviour				**Sliding behaviour**	
	Shear modulus	**Failure criterion**	τ_0	μ_d	**c**	μ_s
Model	**[MPa]**		**[MPa]**		**[MPa]**	
M1,M2,M3	830	Mohr-Coulomb	0.336	0.3	0.336	0.3
M4	830	-	-	-	0.336	0.3

3.1. Non-linear static analyses

This section investigates the structural response of macro- and mesoscale masonry representations by performing nonlinear static analyses. In the simulations, lateral loads, distributed proportional to the mass, were applied and monotonically increased in the positive X direction.

Fig. 4 compares the capacity curves obtained with the mesh mentioned above discretisations and with a homogeneous model performed in Abaqus (Abaqus, 2014), where the nonlinear behaviour of masonry was simulated by means of the concrete damage plasticity model (CDP). One can note how models M1, M2, M3 show small differences in terms of initial stiffness and peak loads, highlighting a slight mesh dependency when a classical DMEM approach is adopted. However, the macroscale representation cannot account for blocks' interlocking, which leads to complex interaction between the macro-elements that involves shear sliding, shear diagonal, torsional, and membrane behaviour. Indeed, the mesoscale model, i.e., M4, provides a stiffer initial behaviour and a higher peak load than the M1, M2 and M3, as a consequence of the misalignment of the vertical interfaces. Moreover, the results demonstrate how stone's interlocking influences the post-peak behaviour. In particular, two drops are shown with the mesoscale discretisation: the first one is due to the crack propagation that starts from the opening in the later wall, while the second drop is linked to the crack propagation at the base of the orthogonal wall without openings, which shows a flexural rocking mechanism in its plane. Consequently, differences in collapse mechanism can be noted in Fig. 5, where model M4 leads to more realistic results.

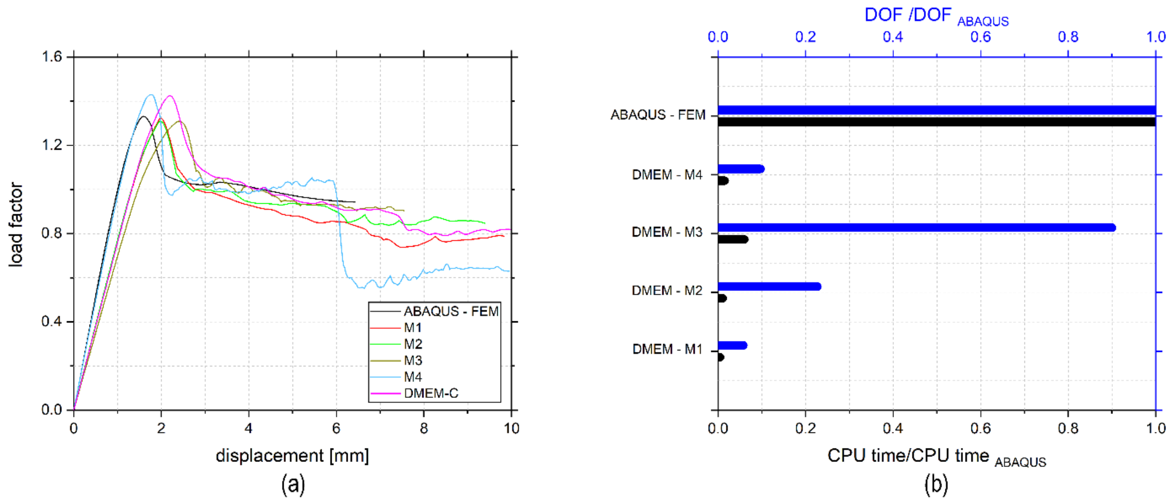

Fig. 4: Nonlinear static analysis for the U-shape stone: (a) Comparison in terms of load-displacement curve; and (b) Normalised computational time (CPU) and normalised number of degrees-of-freedom (DOFs).

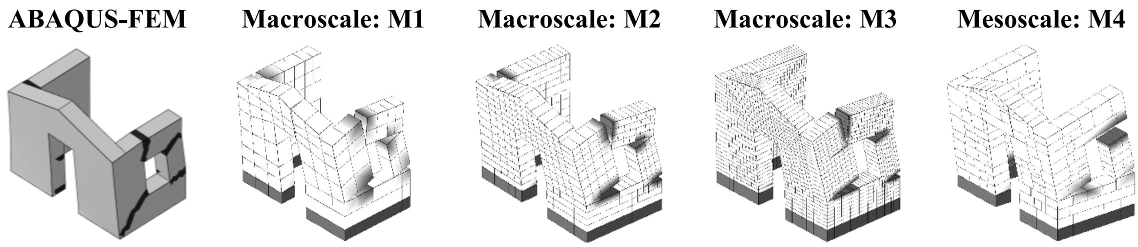

Fig. 5: Comparison in terms of failure mechanisms.

According to Pantò et al. (2019), the tensile strength and fracture energy must be recalibrated to take into account the over-strength effect provided by interlocking using a macroscale discretisation. Hence, an updated macroscale model (DMEM-C) was generated by considering the same mesh discretisation adopted for M1 and a value of 0.240 MPa and 0.060 N/mm for the tensile strength and fracture energy, respectively (see Fig. 4a). The updated macroscale model shows a much better correlation with the results from the mesoscale model.

It is worth underlining how the DMEM approach strongly reduces the computational demands (see Fig. 4b). It has also been observed that mesoscale representation may be a powerful alternative to model unreinforced masonry structures within a DMEM approach (particularly if compared with classic homogeneous FE methodologies).

4. Numerical Investigation: box prototype

In this section, the influence of the irregular masonry pattern on the structural response of a masonry prototype is investigated (see Fig. 6). Two classes of mesh discretisation (A and B) have been generated by using a tool implemented in a GHPython script (*Grasshopper*; *The Python Language Reference)*. Each subcategory is characterised by a different number of the unit's row equal to (A) 18 and (B) 12, respectively. For both classes, five masonry patterns have been generated with increasing levels of randomness and with or without the presence of openings (Fig. 7).

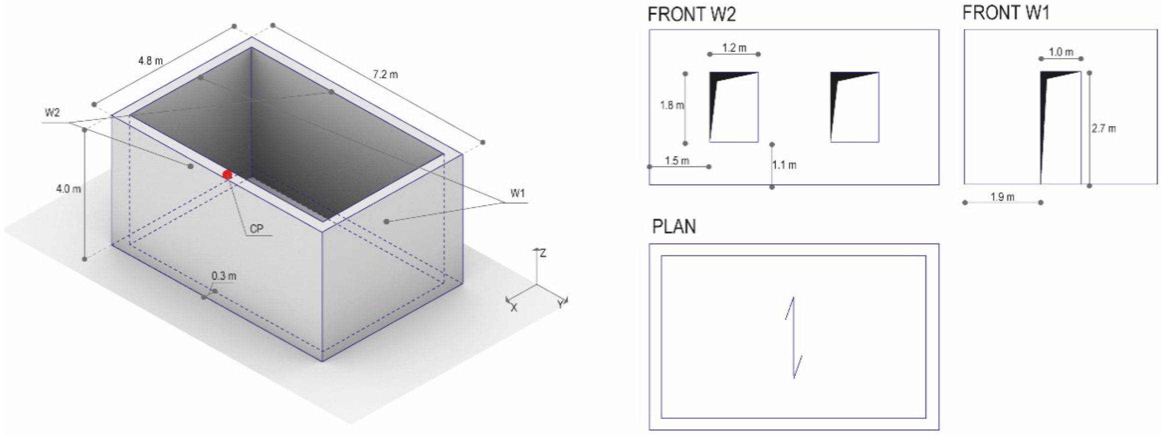

Fig. 6: Parent geometry for box prototype: geometrical features.

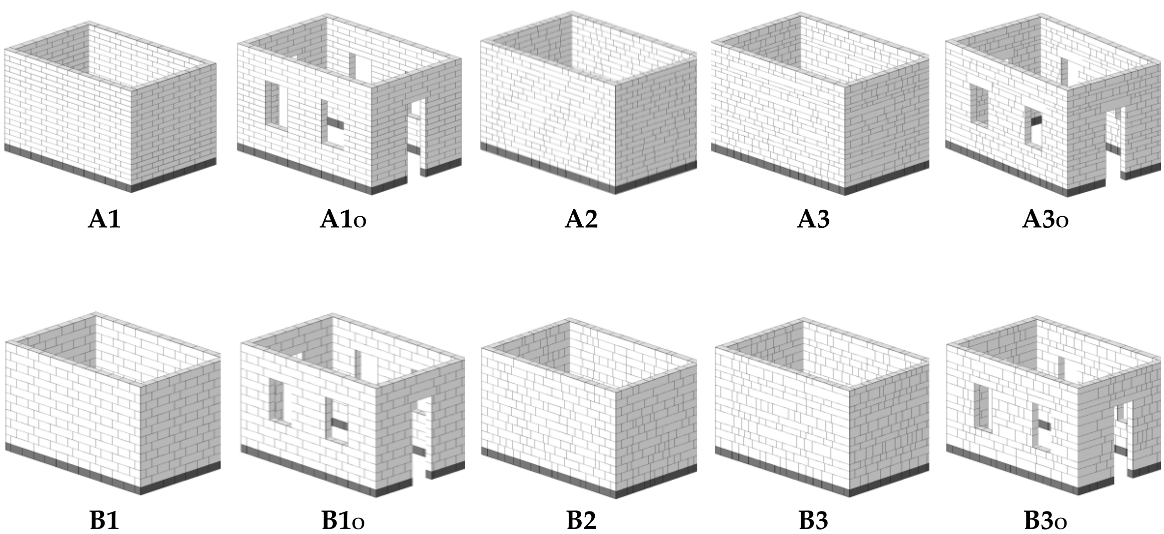

Fig. 7: Mesh discretisations adopted for the box prototype with a total of ten different geometries.

Table 3 and Table 4 summarise the mechanical properties adopted across the numerical simulation. The tensile strength and fracture energy have been assumed to be extremely small to simulate dry-stacked masonry.

Table 3: Mechanical properties adopted for the box prototype: flexural behaviour

	Flexural behaviour					
	Density	**Young's modulus**	**Compressive strength**	**Compressive fracture energy**	**Tensile strength**	**Tensile fracture energy**
Model	**[kg/m^3]**	**[MPa]**	**[MPa]**	**[N/mm]**	**[MPa]**	**[N/mm]**
Mesoscale	1800	1500	3.80	3.00	0.001	0.0001

Table 4: Mechanical properties adopted for the box prototype: shear behaviour

	Diagonal cracking behaviour				Sliding behaviour	
	Shear modulus	**Failure criterion**	**τ_0**	**μ_d**	**c**	**μ_s**
Model	**[MPa]**		**[MPa]**		**[MPa]**	
Mesoscale	580	-	-	-	0.001	0.6

4.1. Nonlinear static analyses

Nonlinear static analyses have been performed applying an incremental lateral load distribution proportional to the mass, in the X+ direction. The results in terms of capacity curves are reported in Fig. 8a and Fig. 8b for classes A and B of mesh discretisation, respectively. One can note how irregular masonry patterns as well as the presence of the openings, tend to decrease the capacity of the structures. Moreover, Fig. 8 provides a comparison between regular mesoscale configurations (A1, B1), irregular models (A2, A3, B2, B3) and a classical macro-element mesh discretisation ($DMEM_A$, $DMEM_B$). To this end, reverse engineering was considered for selected mechanical parameters to get a good match in terms of structural response between macroscale and mesoscale models. In order to simulate the interlocking effect, in the macroscale model, the shear-diagonal behaviour has been calibrated according to a Turnsek-Cacovic failure criterion assuming a perfectly post-elastic law.

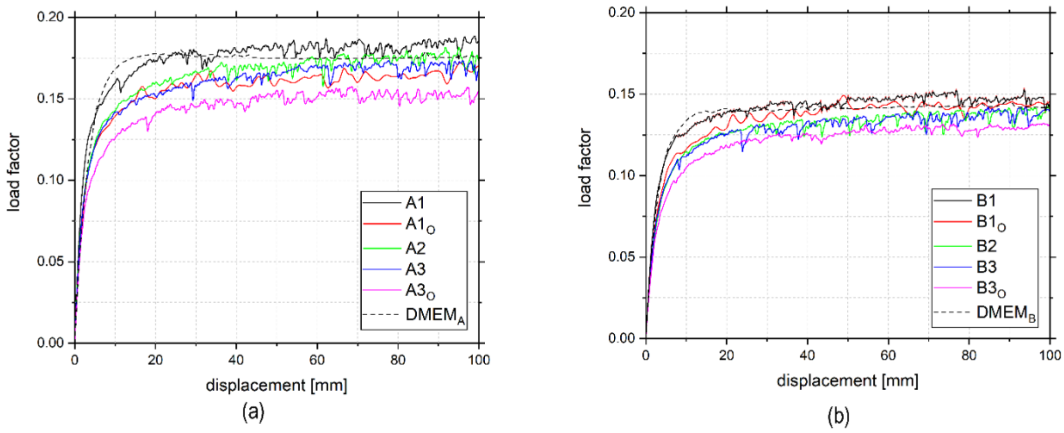

Fig. 8: Comparison in terms of load-displacement curves for classes A and B characterised by a number of units' courses equal to: (a) 18 and (b) 12.

The shear strength in the absence of axial load has been assumed to be equal to 0.2 MPa while a value of 0.6 has been considered for the friction coefficient μ_s. The tensile strength f_t and the cohesion c, which affected the peak of the capacity curve, have been increased to 0.025 MPa in macro-model A and to 0.015 MPa in macro-model B with the aim to satisfactorily reproduce the static nonlinear response of the mesoscale models A1 and B1, respectively. Moreover, the value of tensile fracture energy G_{ft}, which influenced the post-peak capacity as reported in Pantò et al. (2019), was increased to 0.25 and 0.30 N/mm in the constitutive law of model A and B, respectively. It is worth noting that the interlocking phenomenon effect on the initial stiffness is less pronounced than the previously analysed U-shape. It happens because the interlocking phenomenon tends to increase the structure's initial stiffness, particularly when the slenderness ratio is small.

4.2. Nonlinear dynamic analyses

In this section, incremental dynamic analysis (IDA) has been performed applying the Amatrice EW (2016) earthquake record as input ground motion in the x-direction (see Fig. 9a). Several scale factors (SF) have been applied to the selected record until reaching the near-collapse condition of the investigated masonry prototype. The numerical procedure for the solution of the dynamic equilibrium was based on the Newmark method assuming $\gamma = 0.5$ and $\beta = 0.25$ (Newmark, 1959) and a time step equal to 0.005 s. Moreover, the energy dissipation was based on a Rayleigh viscous damping criterion where a value of 5% of the damping ratio has been associated with the 1st and 10th natural frequencies.
The results in terms of normalised maximum horizontal displacement of the control point $u_{max}/u_{max,abs}$ are reported in Fig. 9b as a function of the scale factor SF. It is worth noting how the influence of the mesh pattern increases with the increase of the scale factor, as highlighted by the divergent behaviour of maximum reached displacement for higher value of PGA.

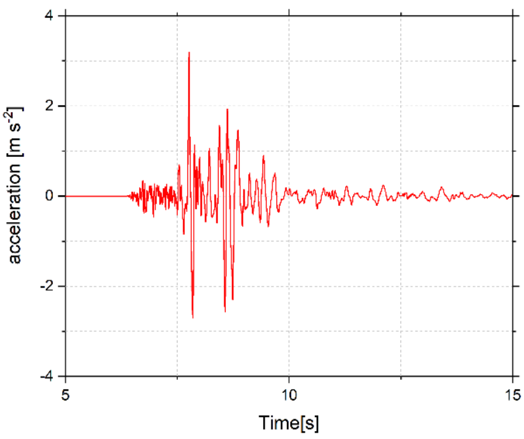

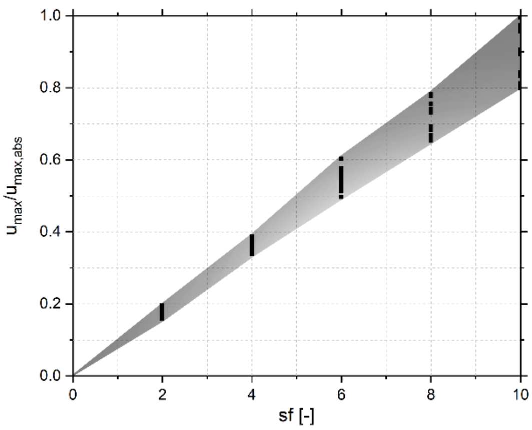

Fig. 9: Nonlinear dynamic analysis: (a) Amatrice EW (2016) record; and (b) ratio between the maximum displacement of the control point and the absolute maximum displacement for all mesh discretisation as a function of the scale factor of the record: envelope of the results.

5. Conclusions

This paper investigated the adoption of a mesoscale representation, rather than a classical macroscale representation, using the DMEM approach. At first, parametric analyses were performed to evaluate the mesh sensitivity and shed light on the mechanical parameters that need to be calibrated to consider physical phenomena, namely interlocking behaviour generated by the vertical joint misalignment. Such investigations were performed by using a benchmark model represented by a U-shape stone masonry prototype, idealising the experimental tests performed at the LNEC shaking table by Candeias et al. (2017). Results

underlined the need to recalibrate the tensile fracture energy as well as the tensile strength. Furthermore, the comparisons with a classical FE homogeneous model show that DMEM requires much lower computational demand, also if the adopted discrete modelling approach contemplated a unit by unit mesoscale modelling.
A total of ten masonry prototypes, with random distribution of regular masonry units, were defined. Both nonlinear static and dynamic analyses were performed and results demonstrate how the masonry pattern affected the structural response. In this regard, it is worth noting that the increase of the randomness degree of masonry units' arrangement can lead to early loss of box behaviour.

References

Abaqus, V. (2014). 6.14 Documentation. *Dassault Systemes Simulia Corporation*, *651*(6.2).

Bui, T. T., Limam, A., Sarhosis, V., & Hjiaj, M. (2017). Discrete element modelling of the in-plane and out-of-plane behaviour of dry-joint masonry wall constructions. *Engineering Structures*, *136*(October), 277–294. https://doi.org/10.1016/j.engstruct.2017.01.020

Caliò, I., Marletta, M., & Pantò, B. (2012). A new discrete element model for the evaluation of the seismic behaviour of unreinforced masonry buildings. *Engineering Structures*, *40*, 327–338. https://doi.org/10.1016/j.engstruct.2012.02.039

Candeias, P. X., Costa, A. C., Mendes, N., Costa, A., & Lourenço, P. B. (2017). Experimental Assessment of the Out-of-Plane Performance of Masonry Buildings Through Shaking Table Tests. *International Journal of Architectural Heritage*, *11*(1).

Cannizzaro, F., & Lourenço, P. B. (2016). Simulation of Shake Table Tests on Out-of-Plane Masonry Buildings. Part (VI): Discrete Element Approach. *Https://Doi.Org/10.1080/15583058.2016.1238973*, *11*(1), 125–142. https://doi.org/10.1080/15583058.2016.1238973

Cannizzaro, F., Pantò, B., Caddemi, S., & Caliò, I. (2018). A Discrete Macro-Element Method (DMEM) for the nonlinear structural assessment of masonry arches. *Engineering Structures*, *168*(October 2020), 243–256. https://doi.org/10.1016/j.engstruct.2018.04.006

Cascini, L., Gagliardo, R., & Portioli, F. (2018). LiABlock_3D: A Software Tool for Collapse Mechanism Analysis of Historic Masonry Structures. *International Journal of Architectural Heritage*, 1–20. https://doi.org/10.1080/15583058.2018.1509155

Chácara, C., Lourenço, P. B., Cannizzaro, F., Pantò, B., & Caliò, I. (2017). *Seismic Assessment of an Unreinforced Masonry Structure Subjected To Out-of-Plane Dynamic Excitations By Means of a Discrete Macro-Modelling Approach*. *July*, 12–15.

D'Altri, A. M., Sarhosis, V., Milani, G., Rots, J., Cattari, S., Lagomarsino, S., Sacco, E., Tralli, A., Castellazzi, G., & de Miranda, S. (2019). Modeling Strategies for the Computational Analysis of Unreinforced Masonry Structures: Review and Classification. *Archives of Computational Methods in Engineering*. https://doi.org/10.1007/s11831-019-09351-x

da Silva, L. C. M., & Milani, G. (2022). A FE-Based Macro-Element for the Assessment of Masonry Structures: Linear Static, Vibration, and Non-Linear Cyclic Analyses. In *Applied Sciences* (Vol. 12, Issue 3). https://doi.org/10.3390/app12031248

de Felice, G., Amorosi, A., & Malena, M. (2010). Elasto-plastic analysis of block structures through a homogenization method. *International Journal for Numerical and Analytical Methods in Geomechanics*, *34*(3), 221–247. https://doi.org/10.1002/nag.799

Felice, Gianmarco de, & Giannini, R. (2001). Out-of-plane seismic resistance of masonry walls. *Journal of Earthquake Engineering*, *5*(2), 253–271. https://doi.org/10.1080/13632460109350394

Fortunato, G., Funari, M. F., & Lonetti, P. (2017). Survey and seismic vulnerability assessment of the Baptistery of San Giovanni in Tumba (Italy). *Journal of Cultural Heritage*, *26*, 64–78. https://doi.org/10.1016/j.culher.2017.01.010

Funari, M. F, Spadea, S., Ciantia, M., Lonetti, P., & Greco, F. (2020). Visual programming for the structural assessment of historic masonry structures. *REHABEND*.

Funari, M., Spadea, S., Lonetti, P., Fabbrocino, F., & Luciano, R. (2020). Visual programming for structural assessment of out-of-plane mechanisms in historic masonry structures. *Journal of Building Engineering*, *31*. https://doi.org/10.1016/j.jobe.2020.101425

Funari, Marco F., Silva, L. C., Savalle, N., & Lourenço, P. B. (2022). (in press) A concurrent micro/macro FE-model optimized with a limit analysis tool for the assessment of dry-joint masonry structures. *International Journal for Multiscale Computational Engineering*. https://doi.org/10.1615/IntJMultCompEng.2021040212

Funari, Marco Francesco, Hajjat, A. E., Masciotta, M. G., Oliveira, D. V., & Lourenço, P. B. (2021). A Parametric Scan-to-FEM Framework for the Digital Twin Generation of Historic Masonry Structures. *Sustainability 2021, Vol. 13, Page 11088*, *13*(19), 11088. https://doi.org/10.3390/SU131911088

Funari, Marco Francesco, Silva, L. C., Mousavian, E., & Lourenço, P. B. (2021). Real-time Structural Stability of Domes through Limit Analysis: Application to St. Peter's Dome. *International Journal of Architectural Heritage*, 1–23. https://doi.org/10.1080/15583058.2021.1992539

Grasshopper - algorithmic modeling for Rhino. (n.d.).

Karimzadeh, S., Kadas, K., Askan, A., Erberik, M. A., & Yakut, A. (2020). Derivation of analytical fragility curves using SDOF models of masonry structures in Erzincan (Turkey). *Earthquakes and Structures*, *18*(2), 249–261.

Lemos, J. V. (2019). Discrete element modeling of the seismic behavior of masonry construction. *Buildings*, *9*(2). https://doi.org/10.3390/buildings9020043

Lourenço, P B, Funari, M. F., & Silva, L. C. (2022). Building resilience and masonry structures : How can computational modelling help ? In G. Meschke, B. Pichler, & J. G. Rots (Eds.), *Computational Modelling of Concrete and Concrete Structures* (1st Editio, pp. 30–37). CRC Press. https://doi.org/10.1201/9781003316404-4

Lourenço, Paulo B., & Silva, L. C. (2020). Computational applications in masonry structures: from the meso-scale to the super-large/super-complex. *International Journal for Multiscale Computational Engineering*, *18*(1), 1–30. https://doi.org/10.1615/IntJMultCompEng.2020030889

Malena, M., Portioli, F., Gagliardo, R., Tomaselli, G., Cascini, L., & de Felice, G. (2019). Collapse mechanism analysis of historic masonry structures subjected to lateral loads: A comparison between continuous and discrete models. *Computers and Structures*, *220*, 14–31. https://doi.org/10.1016/j.compstruc.2019.04.005

Malomo, D., & DeJong, M. J. (2021). A Macro-Distinct Element Model (M-DEM) for simulating the in-plane cyclic behavior of URM structures. *Engineering Structures*, *227*(April 2020), 111428. https://doi.org/10.1016/j.engstruct.2020.111428

Maria D'Altri, A., Lo Presti, N., Grillanda, N., Castellazzi, G., de Miranda, S., & Milani, G. (2021). A two-step automated procedure based on adaptive limit and pushover analyses for the seismic assessment of masonry structures. *Computers and Structures*, *252*, 106561. https://doi.org/10.1016/j.compstruc.2021.106561

Newmark, N. M. (1959). A Method of Computation for Structural Dynamics. *Journal of the Engineering Mechanics Division*, *85*(3), 67–94. https://doi.org/10.1061/JMCEA3.0000098

Pantò, B., Silva, L., Vasconcelos, G., & Lourenço, P. B. (2019). Macro-modelling approach for assessment of out-of-plane behavior of brick masonry infill walls. *Engineering Structures*, *181*(November 2018), 529–549. https://doi.org/10.1016/j.engstruct.2018.12.019

Pantò, Bartolomeo, Giresini, L., Sassu, M., & Caliò, I. (2017). Non-linear modeling of masonry churches through a discrete macro-element approach. *Earthquake and Structures*, *12*(2), 223–236. https://doi.org/10.12989/eas.2017.12.2.223

Quagliarini, E., Maracchini, G., & Clementi, F. (2017). Uses and limits of the Equivalent Frame Model on existing unreinforced masonry buildings for assessing their seismic risk: A review. *Journal of Building Engineering*, *10*, 166–182. https://doi.org/10.1016/j.jobe.2017.03.004

Sarhosis, V., Lemos, J. V, & Bagi, K. (2019). Chapter 13 - Discrete element modeling. In B. Ghiassi & G. B. T.-N. M. of M. and H. S. Milani (Eds.), *Woodhead Publishing Series in Civil and Structural Engineering* (pp. 469–501). Woodhead Publishing. https://doi.org/https://doi.org/10.1016/B978-0-08-102439-3.00013-0

Savalle, N., Lourenço, P. B., & Milani, G. (2022). Joint Stiffness Influence on the First-Order Seismic Capacity of Dry-Joint Masonry Structures: Numerical DEM Investigations. *Applied*

Sciences, *12*(4), 2108.
Savalle, N., Vincens, É., & Hans, S. (2020). Experimental and numerical studies on scaled-down dry-joint retaining walls: Pseudo-static approach to quantify the resistance of a dry-joint brick retaining wall. *Bulletin of Earthquake Engineering*, *18*(2), 581–606. https://doi.org/10.1007/s10518-019-00670-9
Sharma, S., Silva, L. C., Graziotti, F., Magenes, G., & Milani, G. (2021). Modelling the experimental seismic out-of-plane two-way bending response of unreinforced periodic masonry panels using a non-linear discrete homogenized strategy. *Engineering Structures*, *242*(December 2020). https://doi.org/10.1016/j.engstruct.2021.112524
Siano, R., Roca, P., Camata, G., Pelà, L., Sepe, V., Spacone, E., & Petracca, M. (2018). Numerical investigation of non-linear equivalent-frame models for regular masonry walls. *Engineering Structures*, *173*, 512–529. https://doi.org/https://doi.org/10.1016/j.engstruct.2018.07.006
Silva, L. C., Lourenço, P. B., & Milani, G. (2020). Numerical homogenization-based seismic assessment of an English-bond masonry prototype: Structural level application. *Earthquake Engineering & Structural Dynamics*, *49*(9), 841–862. https://doi.org/10.1002/eqe.3267
Silva, L. C., Mendes, N., Lourenço, P. B., & Ingham, J. (2018). Seismic Structural Assessment of the Christchurch Catholic Basilica, New Zealand. *Structures*, *15*, 115–130. https://doi.org/10.1016/j.istruc.2018.06.004
Szabó, S., Kövesdi, A., Vasáros, Z., Csicsely, Á., & Hegyi, D. (2021). The cause of damage and failure of the Mud-brick vault of the Khan in New-Gourna. *Engineering Failure Analysis*, *128*, 105567. https://doi.org/10.1016/J.ENGFAILANAL.2021.105567
The Python Language Reference — Python 3.9.5 documentation. (n.d.).
Vadalà, F., Cusmano, V., Funari, M. F., Caliò, I., & Lourenço, P. B. (2022). On the use of a mesoscale masonry pattern representation in discrete macro-element approach. *Journal of Building Engineering*, *50*, 104182. https://doi.org/https://doi.org/10.1016/j.jobe.2022.104182